

UDK: 573.311.3; 622.785

Novel Method for Measurement of Pipeline Materials Fracture Resistance-Examination on Selective Laser Sintered Cylindrical Specimens

Isaak Trajković^{1*}, Miloš Milošević¹, Milan Travica¹, Marko Rakin², Goran Mladenović³, Ljudmila Kudrjavceva⁴, Bojan Medjo²

¹Innovation Center of the Faculty of Mechanical Engineering, Kraljice Marije 16, 11120, Belgrade, Serbia.

²University of Belgrade, Faculty of Technology and Metallurgy, Karnegijeva 4, 11120, Belgrade, Serbia.

³University of Belgrade, Faculty of Mechanical Engineering, Kraljice Marije 16, 11120, Belgrade, Serbia.

⁴State University of Novi Pazar, Vuka Karadžića bb, Novi Pazar, 36300, Serbia.

Abstract:

This paper presents a part of development of a non-standard method for testing of cylindrical test specimens for measurement of fracture properties of pipeline materials. This method for testing of cylindrical structures working under pressure is based on determining of fracture mechanics parameters on SENT (Single Edge Notched Tension) specimens and new PRNT (Pipe Ring Notched Tension) specimens. In this work, both types of specimens required for this testing were manufactured from polyamide PA12 by using SLS (selective laser sintering) additive manufacturing method. Testing of the specimens is performed on the universal device for testing of mechanical properties of materials Shimadzu, AGS-X 100 kN. The tensile testing is accompanied by GOM Aramis 2M system, used for digital image correlation. By using these two systems, test results are obtained for ring-shaped and SENT specimens, including forces, displacements and fracture mechanics parameters CMOD (Crack Mouth Opening Displacement) and CTOD- δ_5 (Crack Tip Opening Displacement obtained by δ_5 technique), as well as crack growth. Repeatability of this process, along with valid result consistency, represent the basis for further development of the new method, including the determining of energy-based fracture mechanics parameters: J integral and stress intensity factor.

Keywords: Selective Laser Sintering; Polyamide; Digital image correlation – DIC; Fracture mechanics; Pipe ring notched tension specimens.

1. Introduction

The process of transporting fluids to their final destination involves its passing through various parts of processing equipment, including boilers, pumps, branches and pipelines. In addition to metallic pipes (with and without seams), pipes made of plastic materials have seen increased use in fluid transportation, as of recently. Leading polymers used for pipelines include commercial modifications of polypropylene (PP), poly(vinyl-chloride) (PVC) and polyethylene (PE). Polyethylene is currently the most commonly used

*) Corresponding author: trajkovicisaak@gmail.com

material for this purpose, since it can withstand pressures above 10 bar, depending on the exploitation conditions and the type of working fluid, [1].

There is a decades-long tendency to improve traditional pipelines made of metals. Polymer pipes have shown good potential as a replacement since they have advantages in terms of long-term failure resistance and flexibility. Polymer pipes are also easier to install and have shown significant advantages in terms of technical performances and in terms of manufacturing [2,3]. One disadvantage of plastic pipelines during exploitation is somewhat increased vulnerability to external damage of the pipeline surface caused by unexpected factors such as mechanical damage due to human factors or machines. Such damage can sometimes drastically shorten the work life of a pipeline, hence it is necessary not only to characterize the mechanical properties of these polymers, but also to investigate their behavior in the presence of sharp defects including cracks.

Having in mind that it was already determined that non-plastic polyamide (PA12) has mechanical properties which are sufficient for pipeline applications (within the working limit of 18 bar, [4,5]), this polymer will be the material used for testing presented in this paper. Testing is performed mainly in order to develop the new non-standard pipeline test method, mainly for thin-walled pipes, whereas the material was selected based on the previously determined benefits of its use in pipelines, for pressurized fluid exploitation. Also, it is convenient for rapid fabrication of specimens and hence this examination can be regarded as a stage in development of procedure for all types of metallic and non-metallic pipelines.

The main issue with fracture resistance testing occurs with metallic thin-walled pipes which, according to standard EN 10216-2, can be manufactured in over 950 variations (in terms of dimensions). Most pipes manufactured according to this standard are not suitable for standard fracture mechanics testing methods (e.g. ASTM E1820), [6,7], mainly due to the thin walls. There are several suggestions in the literature for development of both new specimen geometries and test methods for non-standard pipeline specimens, [8-13]. Clearly, this is a topic which attracts the attention of the researchers worldwide.

The basis for the introduction of new PRNT (Pipe Ring Notched Tension) samples is found in the work of Gubeljak and Matvienko [14,15], who developed a new non-standard form of samples for pipeline testing. This is the so-called PRNB (Pipe Ring Notched Bending) specimen. Since then, the work has continued on the development of PRNB samples by research groups that have dealt with the integrity of pressurized pipelines through studies based on ring specimens fracture analysis, [16-22]. These studies include experimental results and results obtained using the finite element method; focus was on the micromechanical analysis of failure, the influence of torsional effects and residual stresses on fracture behavior.

Unlike majority of the previously developed specimen geometries, PRNB specimens have the crack position in the longitudinal direction, i.e. the direction which is considered critical for internal pressure loading. As mentioned before, this type of specimen is the base for development of PRNT specimen which tends towards changing of the stress and strain fields, i.e. which tends to approximate the internal pressure through introduction of tensile loading, as opposed to bending applied in case of PRNB specimens.

Having in mind all the mentioned aspects, it can be said that this work is a contribution to development of the new testing method for determining the fracture resistance of the pipeline materials based on the ring-shaped tensile specimens.

2. Materials and Experimental Procedures

2.1. Selective laser sintering – SLS

As mentioned previously, for the purpose of rapid development of the method itself, as well as the specimen design, this research includes testing of PRNT and SENT specimens

fabricated by selective laser sintering, SLS. Selective laser sintering represents an additive manufacturing technique for producing objects from polymer materials in powder form. It holds a formidable position in terms of additive manufacturing techniques since it has the possibility of creating objects “without supports”, which makes it one of the most popular techniques. It is based on powder fusion in layers, whose sintering is done by using energy provided by high-power lasers, which melt the powder in each passing (by bonding via molecular diffusion), [23,24].

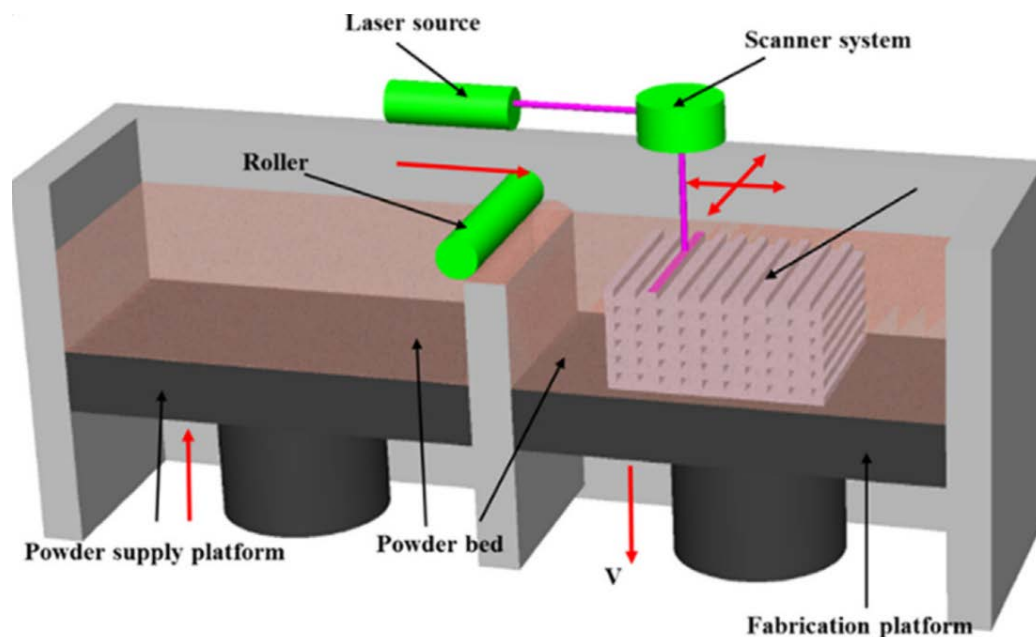


Fig 1. Schematic display of SLS device assembly and working principle [10].

SLS technique is mainly used for rapid product development, along with other additive manufacturing techniques (FDM - fused deposition modeling, SLA - stereolithography, DLP - digital light processing, LM - laser melting). Unlike the usual factors which limit the possibilities of manufacturing complex geometric shapes which are present in conventional techniques, SLS does not suffer from this issue (the use of several machines or special tools). This technique is characterized by lower manufacturing temperatures and lower laser power compared to the LM technique, [25,26].

Materials used for this type of additive manufacturing include thermo-plastic polymers. This means that, in theory, every powdered polymer which behaves as thermo-plastic could be used for the creation of physical models via SLS. The potential issue is the factor related to material selection upon which selective laser sintering technique is based, which is the molecular diffusion process that occurs during the sintering, [27,28].

Modern day commercial applications mostly rely on polycaprolactone (PCL) and polyamide (PA). Polyamide is the leader in commercial systems, both in the form of PA12 compounds and dry mixes with particles such as glass. Polyamide PA11 is a close ‘relative’ of PA12, which has, despite good properties during manufacturing, shown only moderate success when used by the SLS technique. Polymers such as polyether ketone (PEEK) or elastomer polymer types such as thermo-plastic polyurethane (TPU) or thermo-plastic elastomer (TPE) are being commercialized for these applications, but still have certain limitations which result in somewhat moderate success rate. In order to expand this technique to the market and achieve new accomplishments, it would require development of semi-

crystalline polymers such as polypropylene (PP) or polyethylene (HDPE, LLDPE) for use in SLS additive manufacturing, [23,29].

Mechanical properties of polyamide PA12 have previously been discussed in the literature [30-36]. The tests were performed with the purpose of determining the effects of orientation during manufacturing by SLS technique, as well as to compare the results to the same material with additional components (aluminum, glass), and to materials with a different chemical composition as their base. In addition to tests performed in order to determine the mechanical properties of this material, fracture mechanics parameters were also determined in accordance with standard procedures, for assessment of the fracture resistance and integrity of the fabricated products, [37-39].

A group of authors from Austria and Germany examined the properties of pipelines fabricated from PA12, [40,41]. They performed CRB (Cyclic Cracked Round Bar) testing of pipelines. The influence of molecular weight on fracture behaviour was also analyzed by the same group. One of the main aims was determination of the Slow Crack Growth (SCG), by using two accelerated test methods, CRB and SH (Strain Hardening).

Selection of materials which have perspective as replacement for steel pipes, as well as increase of application of rapid production techniques, will contribute to significance of the research results presented in this paper.

2.2. Specimens and testing procedure

As mentioned before, experimental testing is performed on ring-shaped specimens with a single crack (PRNT) and SENT specimens, fabricated by selective laser sintering. The device used for their manufacturing was EOS Formiga P100 (EOS GmbH, Munich, Germany), using Polyamide PA12 (PA 2200 powder); its mechanical properties are given in Table I. The parameters of the SLS process were: laser power 30W, working temperature 170°C, scanning speed 1,6-5 m/s.

Tab. I Polymer PA12 properties. [33]

Property	Value
Tensile Strength	51.2 MPa
Sintered Density	0.95 Kg/dm ³
Young's Modulus of elasticity	2171 MPa
Elongation at break	15.6%

After the specimens were fabricated, remaining powder had to be removed from the models, to keep them clean. Removal of leftover powder is performed using compressed air and a soft brush. Powder located in the sintering chamber can be combined with unused powder in various proportions for further use, depending on the required mechanical properties of the material [42-44].

For the purpose of the tests presented in this paper, two types of specimens were made, each including three specimens with dimensions given in Table II. Fig. 2 shows a drawing of PRNT and SENT specimen with marked dimensions. Figs 3 and 4 show the appearance of the fabricated specimens, respectively. Both types of specimens have the same cross section area (i.e. thickness, width and sharp notch length) and printing direction. The sharp notches on the specimens were cut by a razor blade.

Tab. II Dimensions of PRNT and SENT type of specimens: D - diameter; L - length; B - groove depth; W - tube width; a - length of groove with applied crack.

Dimensions	Ring diameter D (mm)	Wall thickness B (mm)	Specimen width W (mm)	Sharp notch length a (mm)
PRNT	42,2	2,3	9,5	3,2
	Length L (mm)	Thickness B (mm)	Specimen Width W (mm)	Sharp notch length a (mm)
SENT	80,0	2,3	9,5	3,2

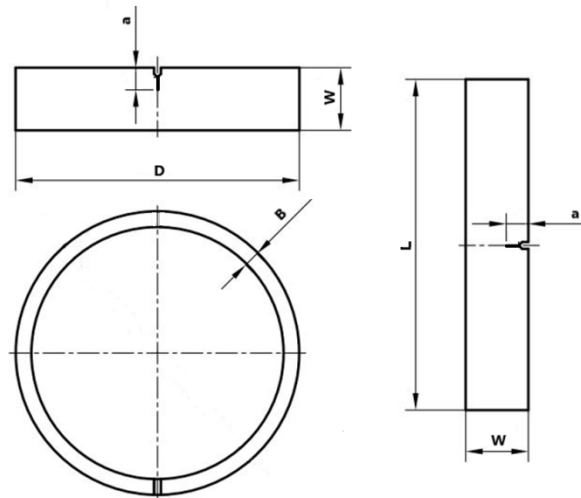


Fig. 2. Drawing with marked dimensions – PRNT and SENT specimen.



Fig. 3. PRNT specimens.

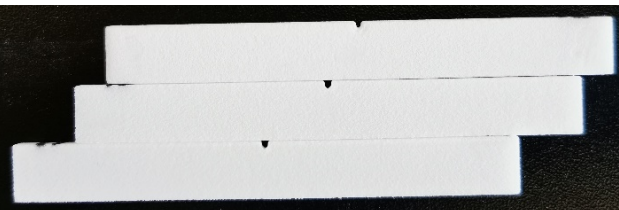


Fig. 4. SENT specimens.

Specimen testing is performed on the universal testing machine Shimadzu (model AGS-X with capacity of 100kN). Supports for plate-shaped specimens with thickness up to 7 mm are used for SENT specimens, in order to fix them within the clamps. Of course, this means that they are tested under fully clamped conditions.

For testing of PRNT specimens, a specially designed and patented tool is used. It consists of two supporting parts and two parts shaped like a half of a cylinder, called the D - blocks, which are placed inside the ring and mounted to the test machine, using the supporting parts. These tools transfer the force to the internal side of the ring, with an aim to simulate the internal pressure, as shown in Fig. 5 [45].

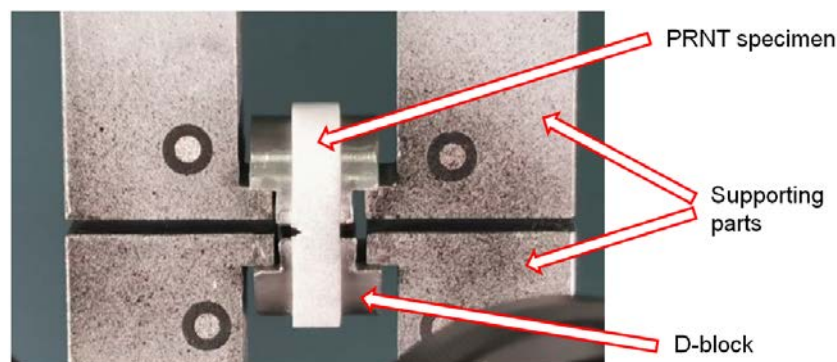


Fig. 5. PRNT specimen and tools for testing.

The tests are performed under displacement control of the device's upper traverse, in the tensile direction, with a rate of 0.5 mm/min, with measuring rate of 10 Hz.

In order to determine the 3D displacements and strains on the specimen surface, as well as geometry fracture mechanics parameters (CMOD and CTOD- δ_5), digital image correlation (DIC) method is used. For the needs of this experiment, GOM Aramis 2M system is applied; it consists of two cameras which work as stereo, the work station (computer), additional lighting using a spotlight and software package for strain analysis.

For proper measurement by digital image correlation, the specimens had to be prepared by applying a stochastic pattern. Considering the matt white color of the specimens in their natural form after manufacturing in the aforementioned way, there was no need to apply white paint, and only a thin layer of finely dispersed spots in matt black is applied by spraying, Fig. 6.



Fig. 6. PRNT specimens with stochastic pattern.

DIC method is based on digitalization of specimen images, prepared as described above, before and after the loading was applied, and based on these images, the system calculates displacements and strains. This represents a standard specimen preparation procedure for this measurement method [46-52].

3. Results and discussion

The results obtained by measurement of force, displacement/strain fields, crack mouth opening displacement CMOD and crack tip opening displacement CTOD- δ_5 , as well as the crack growth, are shown in this section.

Figs 7 and 8 show the results of measurement on specimens PRNT and SENT (respectively), using Shimadzu test machine. The trends of the force-load line displacement curves are similar, and somewhat larger displacements are characteristic for the ring specimens. This may be attributed to the testing setup for SENT specimens, because fully clamped conditions can influence the constraint conditions.

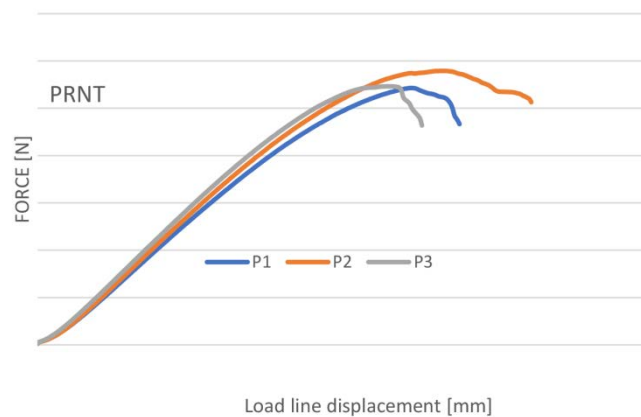


Fig. 7. Dependence of force on the load line displacement for PRNT specimens.

Fig. 8 shows force-displacement dependence for SENT type specimens. Just like the previous figure, it indicates a rather good repeatability of the results up to the maximum force, wherein a difference in specimen behaviour was observed when failure has been initiated. Parts of Figs 7 and 8 after reaching maximum values indicate certain irregularities which can be attributed to specimen manufacturing technique. In this sense, after the maximum force was reached, material failure occurs, wherein the irregularity of failure is the consequence of strength non-homogeneity in material layers. This phenomenon can be much more prominent in other additive manufacturing technologies.

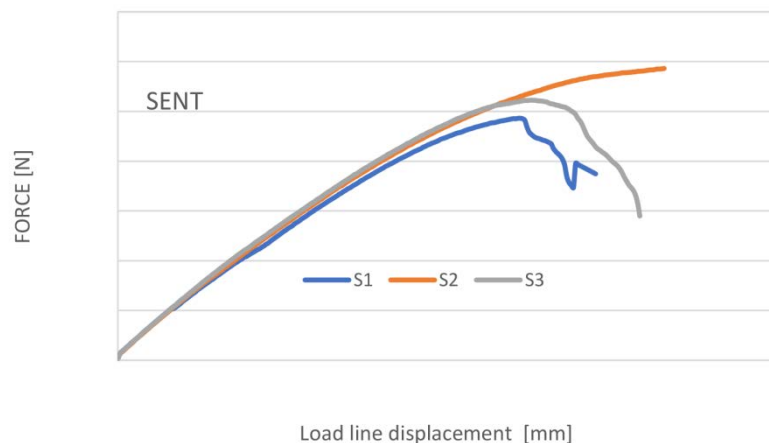


Fig. 8. Dependence of force on the load line displacement for SENT specimens.

Fig. 9 shows an example of report from the Aramis DIC software on which the displacements of the sample surface during loading are measured (vertical displacement is considered here). In the top left part, vertical displacement along the pre-defined vertical sections (0-4) defined by two inclined lines is shown. The trends are very similar, and the curves intersect around the middle of the section length. The sections 0-4 are positioned at equal distances, from the initial notch tip to the right surface of the specimen (opposite to the sharp notch). In the lower left part of Fig. 9, displacements of the three points (stage points 0, 1 and 2) during the loading stages are shown; one stage is recorded every 2 seconds. The trends are linear until the stage 88 (approx. 1.46 mm load line displacement). After that, the displacement of points on upper and lower boundary (0 and 1) deviate from linearity, this can be seen as beginning of nonlinear material behaviour.

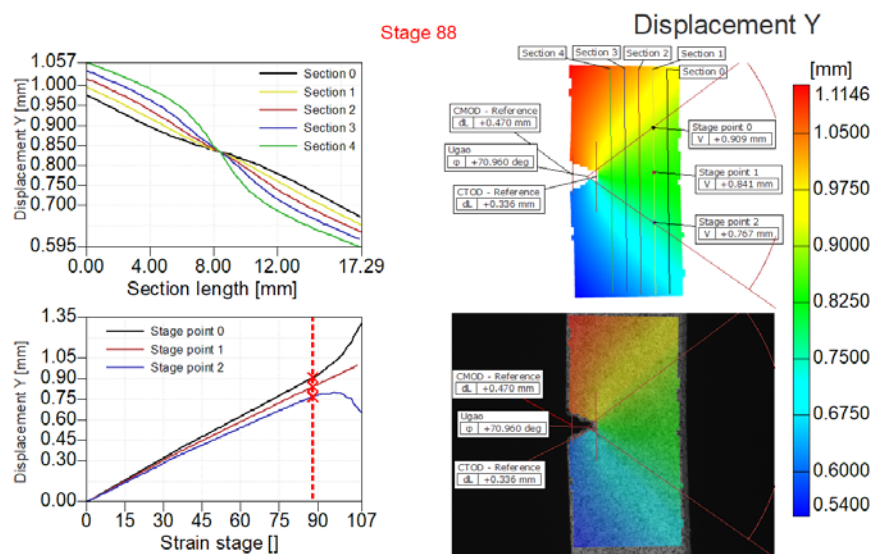


Fig. 9. Report from Aramis system software for SENT specimen.

The values of CMOD (crack mouth opening displacement) and CTOD- δ_5 (crack tip opening displacement) are measured on both PRNT and SENT specimens, by tracking the positions of the points shown in Figure 10 with the increase of external loading. The points for CTOD- δ_5 are initially at the distance of 5 mm.

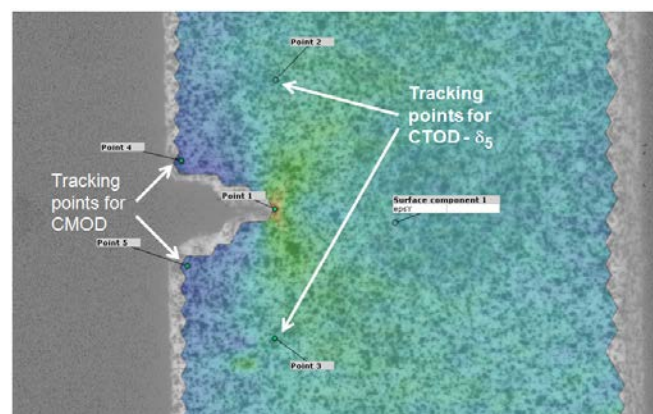


Fig. 10. Strain field obtained by DIC and measurement points for CMOD and CTOD- δ_5 .

Measured CMOD values are shown in Fig. 11, in the form of force vs. CMOD dependence for one SENT and one PRNT specimen. Maximum CMOD value measured on PRNT specimens is 1.1 mm, while the value for SENT specimen is around 1.4 mm. Similar dependences can be seen in Fig. 12, where dependence of the force on crack tip opening displacement (CTOD- δ_5) is given. In both of these figures, the force for the ring specimens is significantly higher, approximately twice, which is caused by the fact that the ring actually has two cross sections and each of them corresponds to the cross section of the SENT specimen. Regardless of the maximum force value differences, both specimen geometries have approximately the same CMOD parameter value of approx. 0.5 mm at maximum force.

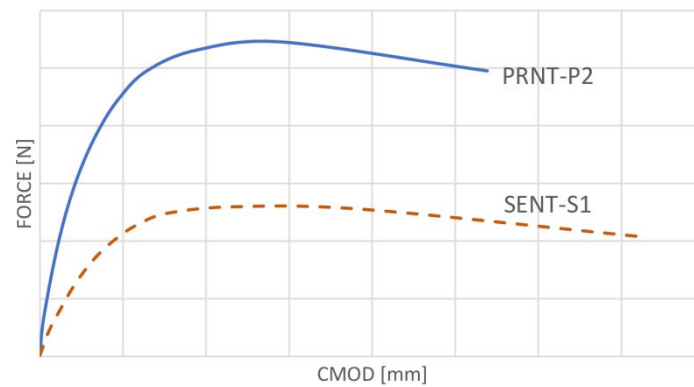


Fig. 11. Dependence of force on CMOD for a PRNT and a SENT specimen.

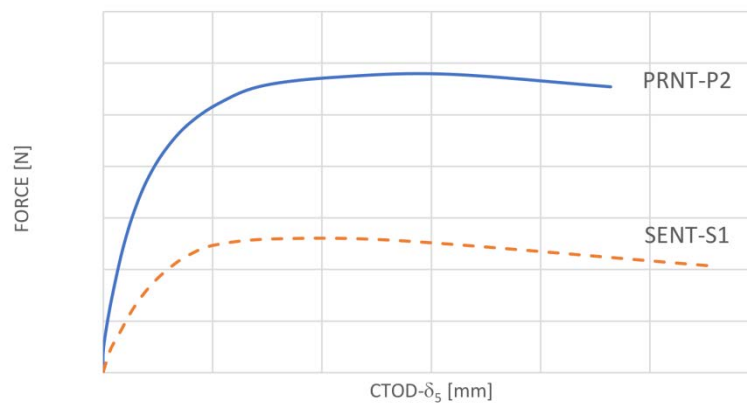


Fig. 12. Dependence of force on CTOD- δ_5 for a PRNT and a SENT specimen.

In addition to tracking of the displacement/strain fields and determining the values of CMOD and CTOD- δ_5 during the testing, digital image correlation is also applied for assessment of the crack growth through the specimen. The criterion for determination of the current position of the crack tip is based on tracking the strain field at the surface, as proposed in [53]. The authors of [53] proposed the strain value 10 % as the criterion for crack growth, while the value 15 % is applied here. In Fig. 13, three stages with the strain fields are shown as an example, and the position of the current crack tip is marked by an arrow in each stage. Of course, due to the excessive deformation and subsequent separation of the material (and its surface black-white pattern), the boundary of the measurement field is moving along with the crack tip growth. As shown in Fig. 13, the strain value 15 % is typically positioned very close to this boundary.

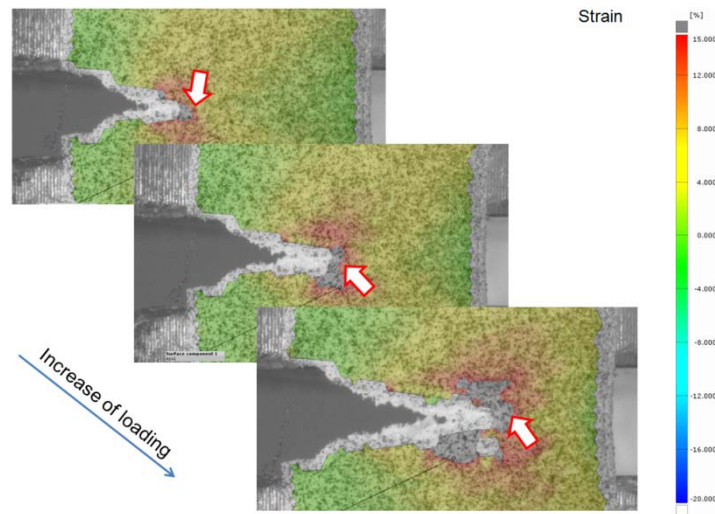


Fig.13. Tracking the crack growth by using the surface strain field (the arrows mark the current crack tip, 15 % strain).

Fig. 14 shows the results of the crack growth tracking, in the form of dependence of crack growth on the load line displacement, for both PRNT and SENT specimen. The obtained difference is consistent with the force-displacement data shown in Figs 7 and 8, and confirms that the crack growth does not occur until the maximum loading is reached. Having in mind that maximum force is obtained later in PRNT specimen, the crack growth also starts later. The criteria for crack growth tracking by application of DIC will be further examined in the future work for different materials, both metallic and non-metallic.

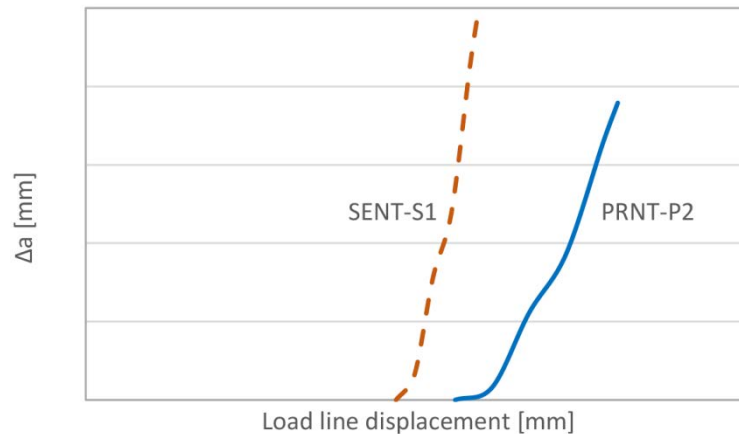


Fig. 14. Crack growth in SENT and PRNT specimens.

During the laboratory analysis performed on specimens obtained by using SLS additive manufacturing technique from polyamide PA12 (PA2200) material, experimental tests have shown the possibility of measuring the necessary quantities on the surface of specimens of both PNRT and SENT geometry, by using Aramis GOM system. Considering the shape of the ring-shaped PRNT specimens, only a three-dimensional system like this could monitor the entire curved measuring surface properly. SLS manufacturing technique used for the selected material shown the possibility of quick manufacturing of specimens with certain structural

non-heterogeneity, which did not result in large deviation in measured force, displacement and strain values in both specimen types.

In this study, production samples with the SLS technique made a significant contribution to the accuracy of the sample geometry, when compared to other additive manufacturing methods. In addition, the production of ring tubes with one groove is very difficult with conventional production techniques. We can conclude that the strategy is well adapted to faster creating of the non-standard testing conditions.

As mentioned before, both specimen geometries have shown repeatable behaviour, i.e. relatively good agreement between the specimens belonging to the same series is obtained. There are certain differences regarding the fracture initiation, i.e. after the maximum force has been reached. Change in material behaviour upon reaching maximum force was a consequence of specimen manufacturing technique which, like other additive manufacturing methods, is characterized by non-homogeneity of specimen structure. Difference in maximum values of CMOD parameter was around 20 % in favour of SENT specimens; however, both specimen geometries exhibit an approximately equal value of CMOD (cca. 0.5 mm) at maximum force. The similarities and differences obtained from these examinations will be taken into account in further development of procedure for experimental fracture testing and post-processing of the results obtained on non-metallic and metallic pipeline materials by application of the pipe ring notched tension specimens.

4. Conclusions

This paper presents the results obtained by examination of SENT (Single Edge Notched Tension) specimens and new PRNT (Pipe Ring Notched Tension) specimens for fracture testing of cylindrical structures such as pipelines. They were fabricated by selective laser sintering from polyamide PA12. Testing of these additively manufactured specimens enabled the setup of a novel testing method for determination of pipeline materials fracture resistance. The results are repeatable, and the same trends are obtained for both types of testing geometries, including the similar values of crack mouth opening displacement CMOD at final fracture. Stereometric strain measurement enabled determination of surface displacement and strain fields, as well as geometry fracture mechanics parameters. Also, it is concluded that stereometric strain measurement can be utilised for tracking of crack growth; however, this will require a detailed analysis for different material groups. For example, higher ductility of the material might affect the value of the surface strain which is used as the criterion for crack growth. Generally, this comparison between the two geometries confirms that the fracture resistance of actual steel or polymer pipes can be determined on newly proposed pipe ring specimens and this examination presents a good basis for further development of the testing and post-processing procedure.

Acknowledgments

The authors acknowledge the support from the Ministry of Education, Science and Technological Development of the Republic of Serbia (contracts: 451-03-68/2022-14/200105 and 451-03-68/2022-14/200135), as well as from Horizon 2020 research and innovation program (H2020-WIDESPREAD-2018, SIRAMM) under grant agreement No 857124. The authors also thank the 3D Impulse Laboratory at the Faculty of Mechanical and Civil Engineering in Kraljevo, University of Kragujevac.

5. References

1. H. Brömstrup, PE 100 Pipe Systems. Vulkan-Verlag GmbH, (2012).
2. L. Janson, *Plastics Pipes for Water Supply and Sewage Disposal*, vol. 4. Stockholm: Majornas CopyPrint AB, (2003).
3. G. Brescia, *The changing World of the Chemical Industry and its impact on the Pipe Industry*. Budapest, Hungary, (2008).
4. M. Hartmann, K. Kuhmann, *Kunststoffe*, 6 (2014) 76-79.
5. M. Hartmann, *KRV Nachrichten*, (2014) 15-17.
6. "ASTM E1820: Standard test method for measurement of fracture toughness, American Society for Testing and Materials,," (2015).
7. "EN 10216-2 - Seamless steel tubes for pressure purposes - Technical delivery conditions - Part 2: Non-alloy and alloy steel tubes with specified elevated temperature properties;," (2002).
8. L. Gajdos, M. Sperl, *Applied Fracture Mechanics*, InTech Publishing, 10 (2012) 283-310.
9. J. M. Koo, S. Park, C. S. Seok, *Nuclear Engineering and Design*, 77 (2013) 198-204.
10. Y. Zhang, P.-Y. ben Jar, *Jurnal Materials and Design*, 77 (2015) 72-82.
11. G. Mahajan, S. Saxena, A. Mohanty, *Fatigue and Fracture of Engineering Materials and Structures*, 39 (2016) 859-865.
12. M. Bergant, A. Yawny, J. Perez Ipiña, *Engineering Fracture Mechanics*, 164 (2016) 1-18.
13. M. Kiraly, D. M. Antok, L. Horvath, Z. Hozer, *Jurnal Nuclear Engineering and Technology*, 50 (2018) 425-431.
14. N. Gubeljak, A. Likeb, Y. Matvienko, *Procedia Materials Science*, 3 (2014) 1934-1940.
15. Y. G. Matvienko, N. Gubeljak, *Model for Determination of crack-resistance of the pipes*, Patent No. RU 2564696 C, (in Russian), (2015).
16. D. Damjanović, D. Kozak, N. Gubeljak, *Engineering Fracture Mechanics*, 205 (2019) 347-358.
17. D. Damjanovic, D. Kozak, I. Gelo, N. Gubeljak, *Theoretical and Applied Fracture Mechanics*, 103 (2019) 102286.
18. W. Musraty, B. Medjo, P. Štefane, Z. Radosavljević, Z. Burzić, M. Rakin, *Chemical Industry*, 72 (2018) 39-46.
19. W. Musraty, B. Medjo, N. Gubeljak, A. Likeb, I. Cvijović-Alagić, A. Sedmak, M. Rakin, *Engineering Fracture Mechanics*, 175 (2017) 247-261.
20. [20] B. Medjo, M. Rakin, N. Gubeljak, Y. Matvienko, M. Arsić, Ž. Šarkoćević, A. Sedmak, *Engineering Failure Analysis*, 58 (2015) 429-440.
21. A. Likeb, N. Gubeljak, Y. Matvienko, *Fatigue and Fracture of Engineering Materials and Structures*, 37 (2014) 1319-1329.
22. B. Medjo, M. Arsić, M. Mladenović, Z. Savić, V. Grabulov, Z. Radosavljević, M. Rakin, *Structural Integrity and Life*, 20 (2020) 82-86.
23. J. P. Kruth, G. Levy, F. Klocke, T. H. C. Childs, *CIRP Annals - Manufacturing Technology*, 56 (2007) 730-759.
24. S. Kumar, *JOM* 55 (2003) 43-47.
25. N. Hopkinson, R. J. M. Hague, P. M. Dickens, *Rapid manufacturing: an industrial revolution for the digital age*. John Wiley, (2005).
26. J. Stašić, D. Božić, *Science of Sintering*, 52, no.1 (202) 15-23.
27. R. D. Goodridge, M. L. Shofner, R. J.M. Hague, M. McClelland, M. R. Schlea, R. B. Johnson, C. J. Tuck, *Polymer Testing*, 30, no. 1 (2011) 94-100.
28. M. Schmid, A. Amado, K. Wegener, *AIP Conference Proceedings*, 1664 (2015).

29. J. R. C. Dizon, A. H. Espera, Q. Chen, R. C. Advincula, Additive Manufacturing, 20 (2018) 44-67.
30. S. Rosso, R. Meneghello, L. Biasetto, L. Grigolato, G. Concheri, G. Savio, Additive Manufacturing, 36 (2020) 101713.
31. D. I. Stoia, E. Linul, L. Marsavina, Materials, 12, 6 (2019) 871.
32. G. V. Salmoria, J. L. Leite, L. F. Vieira, A. T. N. Pires, C. R. M. Roesler, Polymer Testing, 31, 3 (2012) 411-416.
33. E. C. Hofland, I. Baran, D. A. Wismeijer, Advances in Materials Science and Engineering, 2017 (2017) 4953173.
34. W. Cooke, R. A. Tomlinson, R. Burguete, D. Johns, G. Vanard, Rapid Prototyping Journal, 17, 4 (2011) 269-279.
35. G. Berti, L. D'Angelo, A. Gatto, L. Iuliano, Rapid Prototyping Journal, 16, 2 (2010) 124-129.
36. W. Zhang, R. Melcher, N. Travitzky, R. K. Bordia, P. Greil, Advanced Engineering Materials, 11, 12 (2009) 1039-1043.
37. D. I. Stoia, L. Marsavina, Procedia Structural Integrity, 18 (2019) 163-169.
38. A. J. Cano, A. Salazar, J. Rodríguez, Engineering Fracture Mechanics, 203 (2018) 66-80.
39. T. Brugo, R. Palazzetti, S. Ciric-Kostic, X. T. Yan, G. Minak, A. Zucchelli, Polymer Testing 50 (2022) 301-308.
40. M. Messiha, B. Gerets, J. Heimink, A. Frank, F. Arbeiter, K. Engelsing, Polymer Testing, 86 (2020) 227-244.
41. M. Messiha, A. Frank, I. Berger, J. H. Evonik, Proceedings of the 19th Plastic Pipes Conference (2018).
42. A. A. M. Damanhuri, A. Hariri, S. A. Ghani, M. S. S. Mustafa, S. G. Herawan, N. A. Paiman, International Journal of Environmental Science and Development, 12, 11 (2021) 339-345.
43. S. Weinmann, C. Bonten, AIP Conference Proceedings, 2289 (2020).
44. A. A. M. Damanhuri, A. S. A Subki, A. Hariri, B. T. Tee, M. H.F.M Fauadi, M. S.F. Hussin, M. S.S. Mustafa, IOP Conference Series: Earth and Environmental Science, 373, no.1. (2019).
45. M. Travica, N. Mitrović, G. Mladenović, A. Milovanović, N. Milošević, M. Milošević, A. Petrović, "Tool for testing ring-shaped specimens," National patent No. 1629, (2019).
46. M. Milošević, N. Milošević, S. Sedmak, U. Tatić, N. Mitrović, Sergej Hloch, Radomir Jovičić, Tehnicki Vjesnik, 23, 1 (2016) 19-24.
47. M. Milošević, N. Mitrović, R. Jovičić, A. Sedmak, T. Maneski, A. Petrović, A. Tarek, Chem. Listy, 106 (2011) 485-488.
48. M. Milošević, V. Miletić, T. Maneski, Chem. Listy, 105 (2011) 751-753.
49. M. Milošević, N. Mitrović, A. Sedmak, 15th IEEE International Conference on Intelligent Engineering Systems, (2011) 421-425.
50. N. Mitrović, M. Milošević, N. Momčilović, A. Petrović, Ž. Mišković, A. Sedmak, P. Popović, Key Engineering Materials, 586 (2014) 214-217.
51. N. Mitrović, M. Milošević, N. Momčilović, A. Petrović, A. Sedmak, T. Maneski, M. Zrilić, Chemické Listy, 106, no. SUPPL. 3 (2012) 402-405.
52. M. Milošević, Procedia Engineering, 149 (2016) 313-320.
53. P. L. Reu, B. R. Rogillio, G. W. Wellman, OSTI report SAND2007-0156C, United States, (2007) 555-556.

Сажетак: Овај рад представља део развоја нестандардне методе за испитивање цилиндричних епрувета за одређивање отпорности према лому материјала цевовода.

Ова метода за испитивање цилиндричних конструкција које су у експлоатацији изложене унутрашњем притиску заснива се на одређивању параметара механике лома на SENT (Single Edge Notched Tension) епруветама и новим PRNT (Pipe Ring Notched Tension) епруветама. У овом раду, оба типа узорака потребна за ово испитивање произведена су од полиамида PA12 применом СЛС (селективно ласерско синтеровање) адитивне методе производње. Испитивање епрувета је урађено на универзалној тањини за испитивање механичких својстава материјала Shimadzu, AGS - X 100 kN. Испитивање је праћено GOM Aramis 2M системом, који се користи за корелацију дигиталних слика. Коришћењем ова два система добијају се резултати испитивања за епрувете облика прстена и SENT епрувете, укључујући силе, померања и параметре механике лома CMOD (Crack Mouth Opening Displacement) and CTOD- δ_5 (Crack Tip Opening Displacement добијен техником δ_5), као и раст прлине. Поновљивост овог процеса, уз конзистентност резултата, представља основу за даљи развој нове методе, која ће обухватити и одређивање параметара механике лома заснованих на енергији: Јинтеграла и фактора интензитета напона.

Кључне речи: Селективно ласерско синтеровање, полиамид, корелација дигиталне слике – DIC, механика лома, Затезне епрувете облика прстена са зарезом.

© 2022 Authors. Published by association for ETRAN Society. This article is an open access article distributed under the terms and conditions of the Creative Commons — Attribution 4.0 International license (<https://creativecommons.org/licenses/by/4.0/>).

